Int J Adv Manuf Technol (2009) 41:504–512
DOI 10.1007/s00170-008-1490-9

ORIGINAL ARTICLE

Control of microstructure shape and morphology in femtosecond laser ablation of imprint rollers

Wenjun Wang · Xuesong Mei · Gedong Jiang

Received: 26 May 2007 / Accepted: 20 March 2008 / Published online: 26 April 2008

Abstract With increasing demand for microstructure shape accuracy for MEMS and optoelectronic devices, controllability of shape and morphology in micro-fabrication has become increasingly crucial. In this paper, the effects of processing parameters on the shape and morphology of microstructures in femtosecond laser fabrication of imprint roller are explored. An optimized fabrication process is proposed to acquire high accuracy microstructures, in which a two-step inclination ablation process and optimal laser focus position are adopted. Adjusting and matching the processing parameters is a basic method to acquire well-defined shapes, but the ablation results indicate that the draft angle of microstructures can only be adjusted in a limited range due to the intensity distribution of laser beam. A two-step inclination ablation process is adopted to increase the draft angle. In the two-step inclination ablation process, the laser beam irradiates the target surface with an angle and the microstructure with a much steeper draft angle forms after the two-step fabrication. Laser focus position is explored as an important parameter affecting the morphology, and an optimal laser focus position is obtained to enhance the ablation quality. By matching the laser fluence and laser focus position, this morphology enhancement method can realize the high-quality ablation of microstructures with a wide range of dimensions without changing the focusing objective lens.

Keywords Femtosecond laser · Ablation · Microstructure · Morphology · Shape · Process control

W. Wang (✉) · X. Mei · G. Jiang
School of Mechanical Engineering, Xi'an Jiaotong University,
Xi'an 710049, China
e-mail: wenjunwang@mail.xjtu.edu.cn

X. Mei
State Key Laboratory for Manufacturing Systems Engineering,
Xi'an Jiaotong University,
Xi'an 710049, China

1 Introduction

As a low-cost and high-efficiency alternative to conventional photolithography, imprint lithography technique has drawn serious attention because it can easily realize pattern transfer [1, 2]. In recent years, the roller imprint technique has been demonstrated as an alternative approach to the flat imprint technique. This imprint technique has the advantages of achieving better uniformity, needing less force, and having the ability to repeat microstructures continuously on a large substrate, which make it possible to fabricate microstructures in MEMS or optoelectronic devices [3, 4].

With the roller imprint technique, the microstructures on the roller surface are transferred onto the resist or other functional material layer in the ratio of 1:1, so the roller fabrication (fabricating microstructures on the roller surface) is difficult, especially as the microstructure with certain shape is needed. In fact, patterning curved surfaces make the conventional 2D micro fabrication technique such as photolithography invalid. Ruchhoeft et al. used ion beam lithography and step and flash imprint lithography to obtain patterns on curved surfaces [5]. Their method includes seven processes and only a small area on the curved surface can be patterned at a time.

In a recent study, femtosecond laser fabrication of photo masks and other micro devices with a direct writing system has been demonstrated [6, 7]. Due to the ultrashort pulse duration of femtosecond laser, heat diffusion into the surrounding material is negligible and the ablation of the material occurs primarily by direct solid-vapor transition, with no remnant molten material on the substrate under proper process conditions [8–11]. These advantages lead to new possibilities for high-quality material ablation with high reproducibility. Thus femtosecond direct-writing fabrication is expected to be a promising technique to fabricate microstructures on a cylindrical surface. However, there are still some problems waiting to be solved when it is used to fabricate imprint rollers. Firstly, microstructures with certain shape may be needed in some micro-electromechanical systems or optoelectronic devices, but it is difficult to acquire microstructures with the draft angle changing from 0° to 90° using traditional laser processing method. Secondly, although femtosecond laser ablation is a near non-thermal process, sometimes the ablation quality does not meet the application requirements especially as high laser fluence is used. So it is necessary to explore fabrication processes to acquire microstructures with various shapes and to improve the ablation quality of microstructures. In this paper, the effect of processing parameters on the shape of microstructures is explored and a two-step inclination ablation process is proposed to acquire microstructures with the well-defined shape. The effect of laser focus position on ablation quality is studied and the results indicate that the ablation quality can be markedly improved by adopting the optimized laser focus position.

2 Experiments

2.1 Experimental methods

Due to the Gaussian distribution of laser intensity, microstructures ablated by femtosecond laser always have tapered cross-sections and rough bottom morphology unless the target material has been cut through. Moreover, the ablation depth and width always vary simultaneously when process parameters change. So, it is difficult to obtain microstructures with the same depth for different widths. In the experiments, a roller with a two-layer structure is adopted to solve these problems. The roller is made of a cylinder as substrate and a metal film or foil as the pattern layer.

Two methods (sticking patterned foil on cylinder and patterning metal-coated cylinder) can be used to fabricate this kind of two-layer roller. In the first method, the needed microstructures with different shapes are formed on a flat metal foil with femtosecond laser ablation and then the patterned metal foil is stuck on the cylindrical substrate surface, as shown in Fig. 1a. Although this method is simple in principle, there are some difficulties in the sticking process. Firstly, the bending of the metal foils features in the sticking process is inevitable, and this kind of bending is fatal to structures especially as the feature dimension reaches sub-micrometer scale. Secondly, it's difficult to realize the seamless butt joint of patterned foil in the sticking process. If the groove is not parallel to the butt joint gap, the microstructures on the roller will become discontinuous. So, this method is suitable to make the roller with microstructures that have the critical dimension of tens of micrometers and are parallel to the roller axis. Furthermore, the re-fabrication of butt joint place is needed after sticking.

Another method, patterning curved surface, is shown in Fig. 1b. We first stick metal foil or sputter metal film on the cylindrical surface. Then microstructures are fabricated on the metal curved surface. A key element of this method is selecting a kind of proper cylinder material, which must have a high ablation threshold. When the ablation threshold of the cylinder material is on the order of joule per cm^2, the metal coating with the depth of a few microns or nanometers could be removed at the laser fluence on the order of micro joule per cm^2 whereas the substrate material is intact. Moreover, curved surface machining is involved in this method.

As a common metal material with high stiffness, strength and fine thermal conductivity (which are needed in roller imprint process), Fe metal was chosen as the target material in the experiments. Steel foils (purity of Fe: 97%) with the thickness of 30 μm were selected for studying the effect of process parameters on the shape and morphology of microstructures. Fe metal-coated fused silica cylinder was used for the fabrication of the imprint roller. The Fe film (purity of Fe: 99.9%) was acquired by magnetron sputtering and has a thickness of 150 nm; the fused silica cylinder has a diameter of 20 mm.

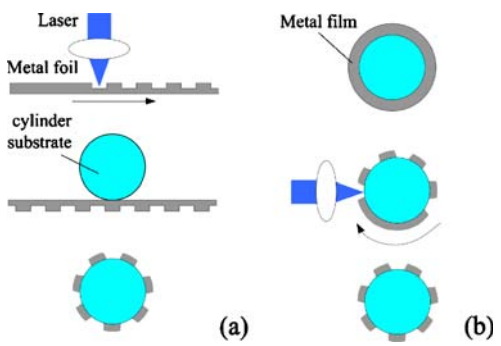

Fig. 1 Sketch diagrams for the fabrication of two-layer structure roller. (**a**) Sticking patterned foil on cylinder. (**b**) Patterning metal-coated cylinder surface

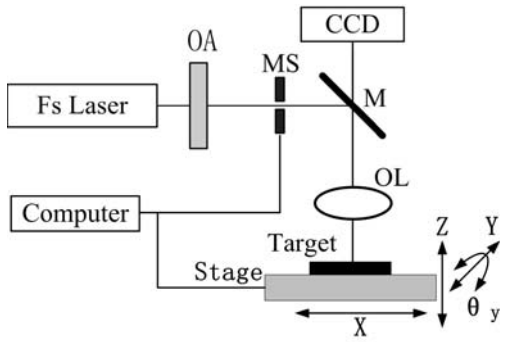

Fig. 2 Schematic illustration of the experimental set-up. OA: optical attenuator, M: mirror, MS: electromechanical shutter, OL: objective lens

2.2 Experiment devices

The experimental setup is illustrated in Fig. 2. Laser ablation experiments were performed in air using a commercially available Ti:sapphire laser system. The laser emitted laser pulses with a wavelength of 800 nm, the pulse duration of 25 fs at a maximum power of 1 W, and a maximum repetition rate of 1 kHz. The target material was mounted on a commercial 3D computer-controlled 10 nm resolution motion stage. The beam was focused onto the target using a microscope objective (NA=0.5) giving a typical focal spot size (r_f=1.6 μm). The output from the femtosecond laser system passed through a continuously variable optical attenuator to control the laser pulse energy. The number of laser pulse exposures was controlled using an electromechanical shutter. A reflecting mirror was used to change the direction of the beam. A CCD camera above the mirror allowed a real-time process observation through the focusing optics. The laser power irradiating on the target surface was measured by a power meter, which has a measuring range of 1 nW ~ 50 mW and measuring accuracy of 0.001 nW.

After laser processing, the samples were subjected to ultrasonic cleaning in methanol for 5 min. The micro-structural characteristics were investigated using a scan electron microscope (SEM) and an atom force microscope (AFM).

3 Effect of processing parameters on the shape of microstructures

When femtosecond laser with certain fluence is used to ablate material, the shape of a microstructure is related to the ablation threshold of material. So the ablation threshold of Fe metal was measured first in our experiments. The ablation threshold of the material for certain number of laser pulses was determined based on the diameter of the ablated area (D) and the corresponding peak laser pulse fluence F [12]. The measured diameter of the ablated area is related to the threshold fluence F_{th} by the following equation,

$$D^2 = 2r_f^2 \ln(F/F_{th}) \tag{1}$$

By extrapolation of D^2 back to zero a value for the ablation threshold fluence, $F_{th}(N)$ can be obtained. There is a reduction in the ablation threshold fluence with increasing incident laser pulse number. The ablation threshold fluence $F_{th}(N)$ for N laser pulses is related to the single-shot ablation threshold fluence by a power law:

$$F_{th}(N) = F_{th}(1)N^{S-1} \tag{2}$$

The incubation coefficient S characterizes the extent to which incubation occurs in the material. Equation (2) can be converted into the following:

$$\ln(N \cdot F_{th}(N)) = \ln F_{th}(1) + S \ \ln \ N \tag{3}$$

It can be seen from Eq. (3) that the logarithm of the product is proportional to ln$N$ with the proportionality coefficient S. The intercept of this line on X-axis is the value of. Using Eq. (1) ~ (3), one can determine ablation threshold of Fe. After experiments and calculation, it is found that the gentle ablation threshold of Fe is 40 mJ/cm^2 with the incubation coefficient S of 0.714 and the strong ablation threshold is 2.07 mJ/cm^2 with the incubation coefficient S of 0.975, shown in Fig. 3.

The scan fabrication used in the experiments is a multi-pulse ablation process, and the relationship of the effective ablation number of laser pulses and scan speed can be given by the following equation:

$$N_{eff} = \sqrt{\frac{\pi}{2}}\frac{2r_f f}{v} \tag{4}$$

where f is the repetition rate of the laser beam, v is the scan speed.

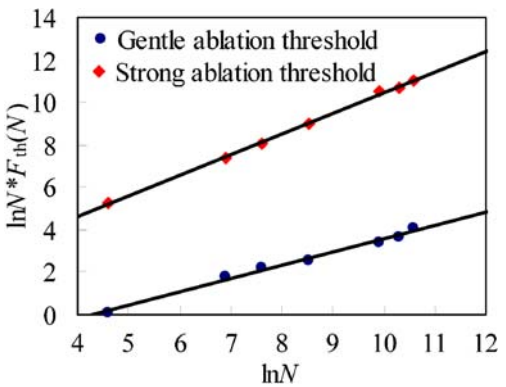

Fig. 3 The curve of incubation effect for Fe. The solid line represents the least-squares fit according to Eq. (3)

The ablation depth of the material is determined by the scan speed and ablation rate L. The ablation rate can be expressed by two different logarithmic functions [8] as:

$$L = \delta \ln\left(\frac{F}{F_{\text{th}}^{\delta}}\right) \tag{5}$$

Or

$$L = \lambda \ln\left(\frac{F}{F_{\text{th}}^{\lambda}}\right) \tag{6}$$

where δ is the optical penetration depth and λ is the heat diffusion length. Here F_{th}^{δ} and F_{th}^{λ} express the gentle ablation threshold and the strong ablation threshold of material, respectively. With a certain ablation rate, the ablation depth is determined by the scan speed. Figure 4 shows the effect of scan speed on ablation depth. The relationship among laser fluence, scan speed and ablation width is expressed by Eqs. (1), (2) and (4). It's clear that the laser fluence has a remarkable effect on ablation width and depth. The number of laser pulses is proportional to the ablation depth, and has little effect on the multi-pulse ablation threshold of material. So scan speed has a serious effect on ablation depth and a slight effect on ablation width, as shown in Fig. 4. As scan speed changed in the range of 0.05 to 1 mm/s, the ablation depth decreased from 10 μm to 2 μm, but the fluctuation of the ablation width was less than 0.5 μm.

The draft angle of a microstructure is another important character of the imprint roller, which is determined by the

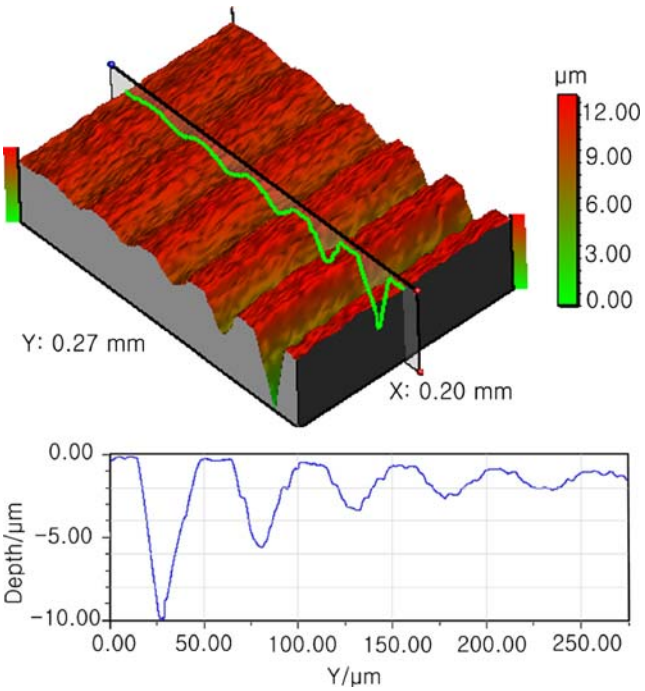

Fig. 4 Surface profile image of microstructures ablated with different scan speed. (left to right: 0.05, 0.1, 0.2, 0.5 and 1 mm/s)

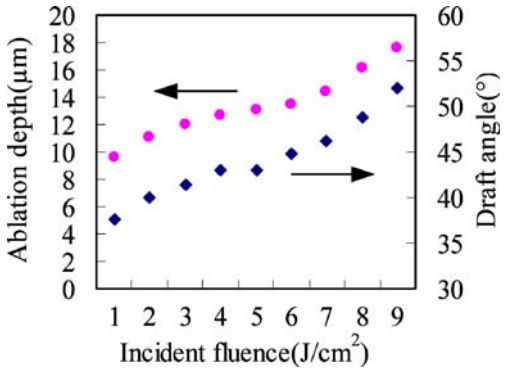

Fig. 5 Dependence of ablation depth and draft angle of microstructures on laser fluence at the scan speed of 0.05 mm/s

width and depth of the microstructure. Figure 5 shows the dependence of ablation depth and draft angle on laser fluence at a scan speed of 0.05 mm/s. The ablation depths of the gentle and strong ablation phases are in proportion to the optical penetration depth δ and the heat diffusion length λ, respectively. In the laser fluence range of 0–5.3 J/cm^2, the ablation depth is low, which is determined by the gentle ablation phase. The ablation depth is experiencing a rapid change at the fluence of 5.3 J/cm^2. After the fluence exceeds 5.3 J/cm^2, the strong ablation phase dominates the ablation process. The draft angle also increases with increasing fluence. The variation of draft angle with fluence is a little different from that of ablation depth due to the influence of ablation width. In general, when the fluence increases from 0 to 9 J/cm^2, the draft angle varies from 37° to 52°. Though different laser fluence will produce different draft angle, it is not advisable to adjust draft angle by changing fluence because not only draft angle but also width of microstructure increases with the increase of fluence. This limits the shape of microstructures seriously.

Figure 6 shows the effect of scan speed on the ablation depth and draft angle. In the laser fluence of 7.6 J/cm^2, the ablation depth is determined by the heat diffusion length λ and the strong ablation threshold of material. In the scan speed range of 0.05–1 mm/s, the ablation depth decreases

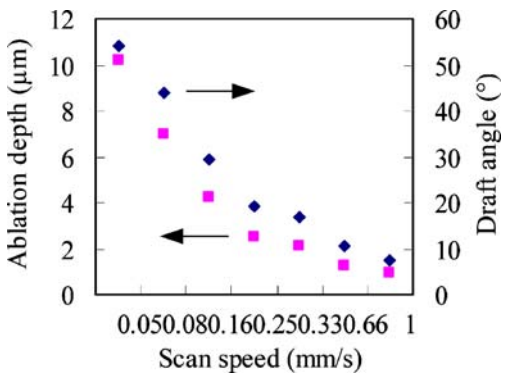

Fig. 6 Dependence of ablation depth and draft angle of microstructures on scan speed with the laser fluence of 7.6 J/ cm^2

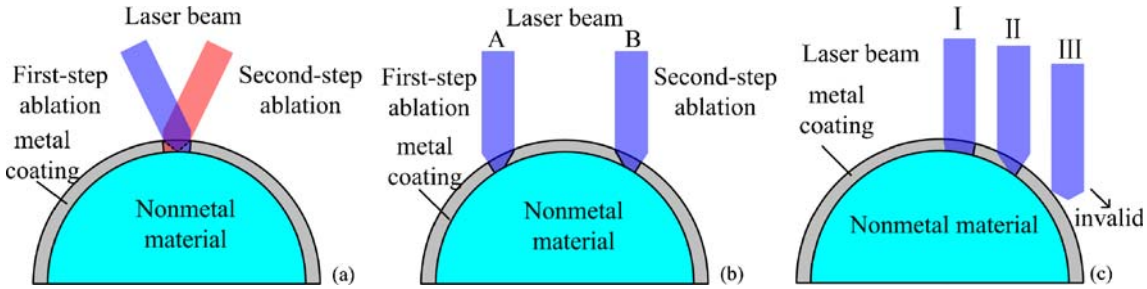

Fig. 7 Sketch of two-step inclination ablation process for fabricating the microstructure with the vertical wall on roller

from 10.2 μm to 0.94 μm and draft angle decreases from 54° to 8°. Changing scan speed is a convenient and effective choice to adjust draft angle of microstructures with almost unchanged width. However, with the increase of pulse number, the ablation depth will reach saturation gradually due to energy coupling, heat conduction, plasma shielding, etc. Thus, the draft angle larger than 60° is difficult to achieve by the optimization of scan speed. Moreover, reducing scan speed will decrease the machining efficiency considerably.

4 Precise microstructure shape control using two-step inclination ablation process

Due to the Gaussian intensity distribution of laser beam, the draft angle of microstructures can only be adjusted in a limited range even if laser fluence and scan speed are optimized. Here a two-step inclination ablation process to realize variable draft angles ranging from 0° to 90° in microstructures with different widths is proposed. In this method, microstructures with a well-defined draft angle can be obtained through changing the relative angle between the laser beam and the target surface.

Figure 7 illustrates the principle of vertical wall fabrication using the two-step inclination ablation of laser beam. Figure 7a shows the realization of the vertical wall through the angled irradiation of laser beam. Another method, laser ablation at different positions of the roller, can also be considered as inclination ablation, shown in Fig. 7b. When the laser beam is fixed on Position A, a microstructure with one sidewall vertical to the roller surface is formed. After all the microstructures on the cylindrical surface are fabricated by rotating, we move the laser beam to Position B, which is symmetrical to Position A, and locate the laser beam focus on the upper surface of the pre-fabricated microstructure using a CCD monitor. Thus the microstructure with vertical walls is formed. Although the two processes shown in Fig. 7a and b are both effective, the process shown in Fig. 7b is easier to realize in the fabrication of cylinder. In this process, the fabricating position to obtain vertical wall is different when different process parameters are used. Figure 7c shows different positions on the roller for obtaining vertical walls with different process parameters in theory. Both Position C and Position D can realize vertical walls with different process parameters. However, Position E is invalid and can not remove the material because the laser is defocused when the beam reaches the target surface. So in inclination ablation, process parameters and fabricating position on the roller have to be selected within a proper range.

Using the two-step inclination ablation process, one can achieve not only the vertical wall but also the other draft angles ranging from 0° to 90°. Via the movement along the

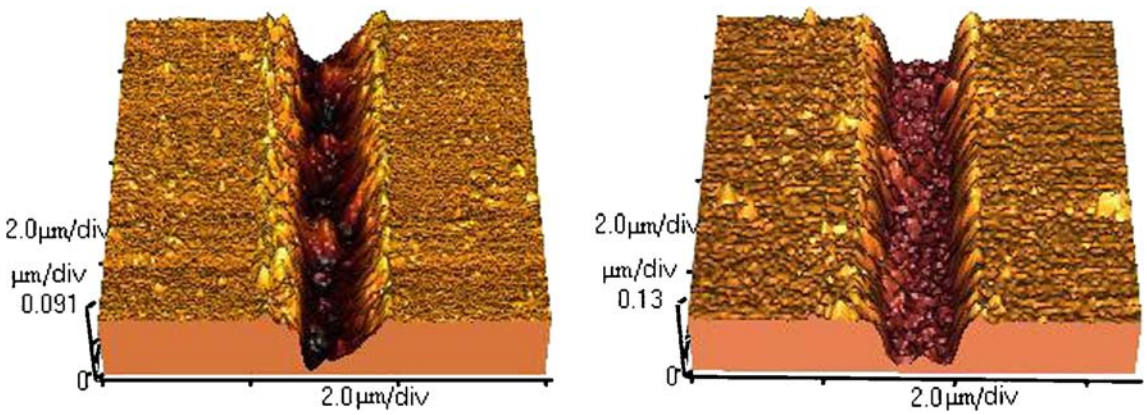

Fig. 8 AFM images of microstructures produced in Fe films, with the scan speed of 0.16 mm/s and the inclination angle of 75° at 10.7 nJ. (**a**) One-step inclination ablation, (**b**) Two-step inclination ablation

horizontal direction of the stage and precise control of rotating angle, this process could be carried out readily. However, the overlap of two microstructures will increase width of the microstructure. This factor should be considered when we determine the appropriate process parameters like laser fluence.

Figure 8 shows the results of inclination ablation in Fe films with the scan speed of 0.16 mm/s at the laser energy of 10.7 nJ. The angles between laser beam and target surface is 75°. The result of one-step inclination ablation is shown in Fig. 8a. The groove has two walls with different draft angles. Figure 8b shows the result of the two-step

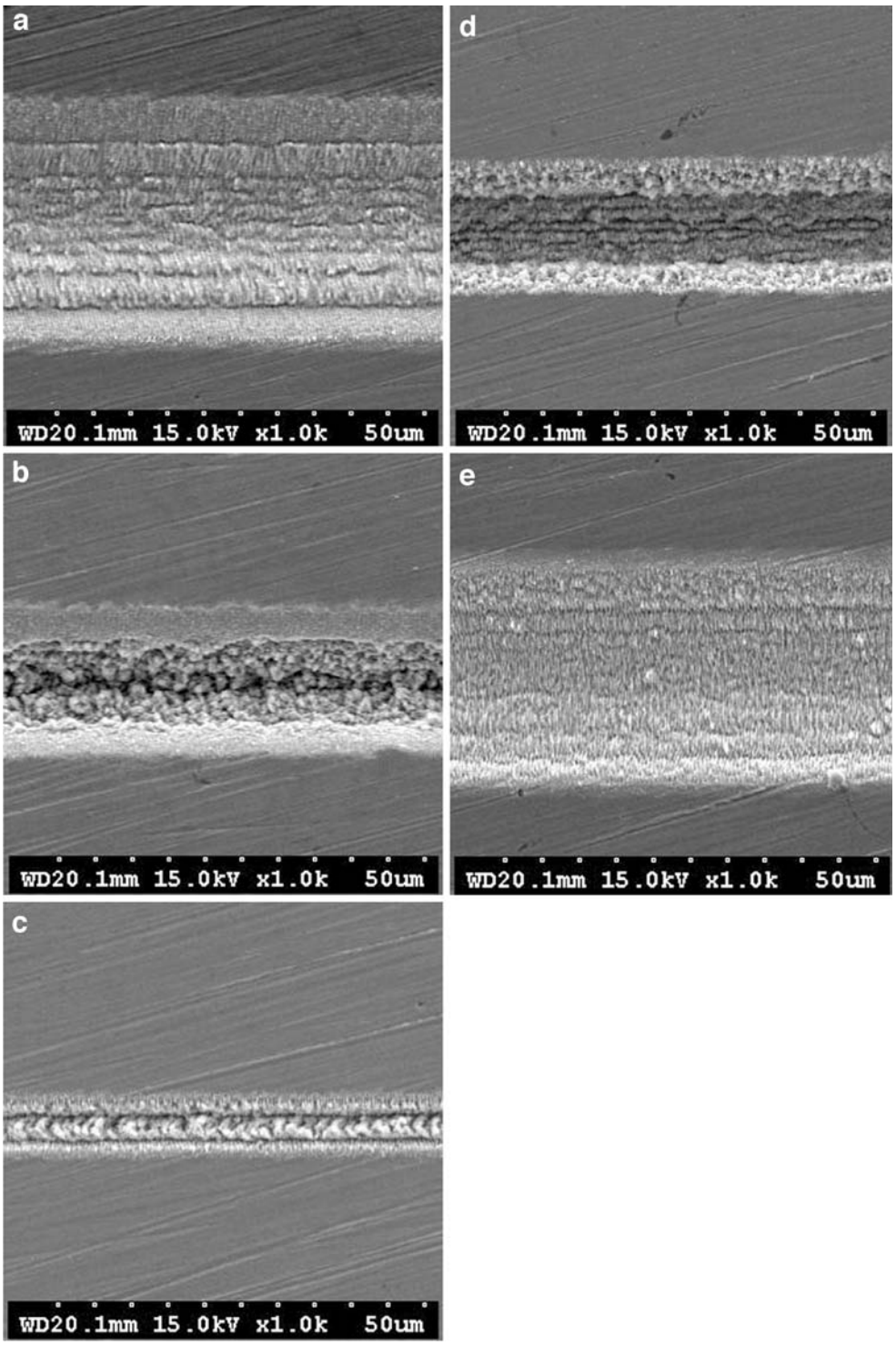

Fig. 9 SEM images of microstructures produced in steel foils, with the scan speed of 0.05 mm/s at 1.9 μJ, the distance from laser focus to target surface is (**a**): -30 μm, (**b**): -15 μm, (**c**): 0 μm, (**d**): 15 μm and (**e**): 30 μm, respectively

inclination ablation. We can find that when two micro-grooves overlap, a new symmetrical micro-groove with certain draft angle is formed. This experimental result demonstrates that inclination ablation can adjust draft angles of microstructures flexibly and effectively.

5 Enhancement of machining quality using optimized laser focus position

In the fabrication of imprint rollers, not only precise shape but also machining quality of the microstructures is important to ensure the imprint quality of the roller. Compared with long pulse laser ablation, femtosecond laser ablation can acquire a better morphology. However, the ablation quality does not meet the demand of application sometimes especially as higher laser fluence is used. So it is necessary to explore the material removing mechanism and adopt an optimized ablation process to improve the structure morphology.

5.1 Material removal mechanism and structure morphology

In femtosecond laser ablation, normal vaporization and phase explosion are the two main material removal mechanisms and the ablation quality of microstructures is mainly dependent on which ablation mechanism acts on. Laser fluence is the processing parameter which determines the transition from normal vaporization to phase explosion. When a lower fluence is used to ablate material, the normal vaporization is the main material removal mechanism. In this situation, because ablated materials transform from solid into vapor directly, no molten layer and resolidified droplets form. So a very smooth ablated surface can be obtained with this kind of material removal mechanism.

With increasing laser fluence, a transition from normal vaporization to phase explosion occurs. Besides the energy used for vaporization, the residual energy in the metal will induce liquid phase of material, which leads to the amorphous phase of the metal during resolidification. If liquid is considerably superheated throughout as compared to the saturation temperature, bubbles of vapor are produced over all the liquid volume, which is phase explosion. As a result of explosive boiling, part of the molten material breaks down into droplets and sputter on the ablated surface. The whole melt layer is abruptly cooled down not to be re-crystallized, but to be amorphous. So the morphology of the ablated surface is poor.

5.2 Optimized laser focus position

As described before, low fluence can prevent the occurrence of phase explosion and acquire high quality microstructures. Adopting proper laser energy and focusing objective lens is a general method to acquire appropriate fluence to create well-defined structure. But replacing objective will bring additional procedures and result in low efficiency. In fact, changing focus position, which can also change the beam spot size, is a convenient alternative method. Laser focus position described here is defined as the distance between the laser focus and the target surface, and the laser focus position above the target surface is defined as the positive direction. In this section, the effect of the laser focus position on the morphology of microstructures is explored and an optimized laser focus position is used to enhance the ablation quality.

In the experiments, to determine the focal plane, the output of the laser was sampled by a CCD camera and attenuated with continuously variable optical attenuator such that the peak response of the camera was the same at each position along the beam path. The laser beam was passed through the focusing lens to the detector which was moved successively along the beam path at an increment of 1 μm. The position where spot size is minimal is regarded as the focal plane. The effect of the laser focus position on dimension and morphology of the microstructures is shown in Fig. 9. These microstructures were ablated with the scan speed of 0.05 mm/s at the energy of 1.9 μJ. From -30 μm to 0, the ablation width decreases and the ablation depth increases gradually. The narrowest microstructure occurs when the laser focuses on the target surface. From 0 to 30 μm, the ablation width increases and the ablation depth decreases again. There is nearly no difference in the ablation width and depth at the symmetrical positions about the focal plane.

Microstructures ablated with different laser focus positions have remarkably different morphologies. Figure 9a and e show a better machining quality. At the focus

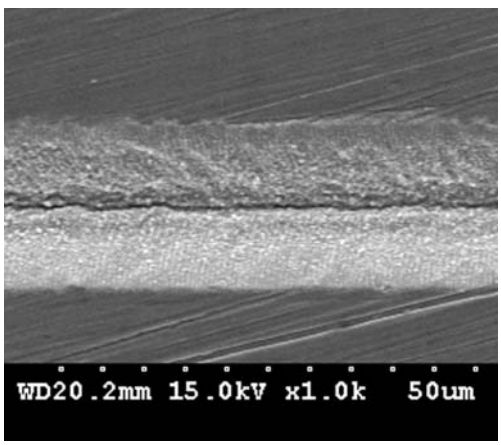

Fig. 10 SEM image of microstructure produced in steel foils, with the scan speed of 0.05 mm/s at 1.4 μJ, the distance from laser focus to target surface is 20 μm

positions of ±30 μm, vaporization is the dominant ablation mechanism in the whole ablated region and phase explosion is absent because of the low laser fluence. The ablation morphology changes obviously when the distance between the focus and the target surface is closer, as shown in Fig. 9b and d. Two kinds of ablation mechanisms occur simultaneously in the whole ablation region. Along the edge of the microstructure, the ablated surface is smooth and flat; while inside the microstructure, the ablated surface is coarse and covered with small droplets. It is noticed that the ablated morphology is worst when the laser just focuses on the target surface, shown in Fig. 9c. Due to the serious phase explosion, a row of surface deposits form inside the ablation region.

In the ideal condition, the distribution of laser energy at both sides of the focus is symmetrical. Thus, for the same spot diameter, the ablation morphology seems to be invariable no matter whether the focus was above or beneath the target surface. However, comparing Fig. 9a with e and Fig. 9b with d, it is found that those microstructures have different ablation morphology. Although microstructures ablated with the focus beneath the target surface have much smoother edges, they still have poorer morphologies compared with that ablated with the focus above the target surface in general. This kind of difference can be attributed to the different beam characteristics in the region of ablation. When the focus is above the ablated surface, the divergent beam is used for ablation; while when the focus is beneath the ablated surface, the convergent beam is used for ablation. In different beam ablations, the changes of spot size and laser fluence irradiated on the ablated surface are distinct. In the diverging beam ablation, with the increase of the ablation pulses, the ablated surface becomes farther away from the focus gradually and the laser fluence on the ablated surface becomes lower and lower; while in the converging beam ablation, the ablated surface approaches the focus gradually and the laser fluence on the ablated surface becomes higher and higher. Because the fluence irradiated on the bottom of grooves in divergent beam ablation is much lower than that in convergent beam ablation, the bottom morphology of the groove ablated with divergent beam is comparatively better than that with convergent beam. Different from the bottoms of the grooves, the edges of the grooves ablated by the divergent beam have worse morphology than those ablated by the convergent beam. In this instance, the material removal mechanism is still vaporization at the edge of groove though the fluence becomes higher in convergent beam ablation, and the worse morphology at edges of grooves ablated with divergent beam ablation can be attributed to the ignition of plasma in the focal region, which locates above the ablated surface and hinders or forces away the eruptible material and eventually cause the redeposition of material on the ablation surface.

Since different laser focus positions lead to the remarkable change of ablation quality, the enhancing method of ablation quality using the optimized laser focus position is as follows: When structures with dimensions of submicron or nanometer are fabricated, the laser beam should focus on the target surface with lower laser energy to ensure the feature size and ablation quality. When the dimension of microstructures is larger, the ablation in focus plane with larger laser energy ceases to be the proper method because it may result in worse ablation quality. In this instance, one approach is to focus laser beam above target surface to weaken the thermal effect and improve the roughness of the ablated surface. However, if the influence of plasma in the focal plane on morphology in divergent beam ablation is serious, the optimized focus position will be beneath the ablation surface with a much lower fluence.

The effect of the optimization of laser focus position is shown in Fig. 10. The microstructure was ablated with the laser focus position of -20 μm at the laser energy of 1.4 μJ. The ablation width of this microstructure is the same as that of the microstructure shown in Fig. 9d. At the same time, due to the ablation mechanism of vaporization, the ablation quality is improved obviously.

6 Conclusions

Process controllability of shape and morphology in femtosecond laser fabrication of microstructures is investigated in this paper. The experimental results indicate that (1) adjusting and matching process parameters can realize microstructures with the draft angle in a range of 0° to 60° easily; (2) the two-step inclination ablation process can increase the draft angle effectively, and this is a promising process for the fabrication of microstructures with vertical sidewalls; (3) adopting the optimal laser focus position can realize the high quality ablation of microstructures with a wide range of dimensions without changing the focusing objective lens.

In fact, the shape and morphology control methods described in this paper can be used to fabricate not only imprint roller, but also other micro devices with different shapes in MEMS and optoelectronic devices.

Acknowledgement The authors would like to acknowledge Shuting Lei for his technical assistance. This work was supported by China's 973 Basics Science Research Program (grant No. 2005CB724106 and 2007CB707703), the National Natural Science Foundation of China (grant No. 50575176 and 50505035), and the New Century excellent personage support plan of the Ministry of Education (grant No. NCET-04–0935).

References

1. Itani T, Suganaga T, Wakamiya W (2004) Total solution in 157 nm lithography for below 65 nm node semiconductor devices. Microelectron Eng 73–74:11–15 DOI 10.1016/S0167-9317(04)00065-6
2. Chou SY, Krauss PR, Renstrom PJ (1995) Imprint of sub-25 nm vias and trenches in polymers. Appl Phys Lett 67:3114–3116 DOI 10.1063/1.114851
3. Tan H, Gilbertson A, Chou SY (1998) Roller nanoimprint lithography. J Vac Sci Technol B 16(6):3926–3928 DOI 10.1116/1.590438
4. Chang CY, Yang SY, Chu MH (2007) Rapid fabrication of ultraviolet-cured polymer microlens arrays by soft roller stamping process. Microelectron Eng 84:355–361 DOI 10.1016/j.mee.2006.11.004
5. Ruchhoeft P, Colburn M, Choi B, Nounu H, Johnson S, Bailey T, Damle S, Stewart M, Ekerdt J, Sreenivasan SV, Wolfe JC, Willson CG (1999) Patterning curved surfaces: template generation by ion beam proximity lithography and relief transfer by step and flash imprint lithography. J Vac Sci Technol B 17(6):2965–2969 DOI 10.1116/1.590935
6. Venkatakrishnan K, Tan B, Stanley P, Lim LEN, Ngoi BKA (2002) Femtosecond pulsed laser direct writing system. Opt Eng 41(6):1441–1445 DOI 10.1117/1.1476324
7. Venkatakrishnan K, Stanley P, Lim LEN (2002) Femtosecond laser ablation of thin films for the fabrication of binary photomasks. J Micromech Microeng 12:775–779 DOI 10.1088/0960-1317/12/6/308
8. Nolte S, Momma C, Jacobs H, Tünnermann A, Chichkov BN, Wellegehausen B, Welling H (1997) Ablation of metals by ultrashort laser pulses. J Opt Soc Am B 14:2716–2722 DOI 10.1364/JOSAB.14.002716
9. Zheng HY, Liu H, Wan S, Lim GC, Nikumb S, Chen Q (2006) Ultrashort pulse laser micromachined microchannels and their application in an optical switch. Int J Adv Manuf Technol 27:925–929 DOI 10.1007/s00170-004-2261-x
10. Knowles MRH, Rutterford G, Karnakis D, Ferguson A (2007) Micro-machining of metals, ceramics and polymers using nanosecond laser. Int J Adv Manuf Technol 33:95–102 DOI 10.1007/s00170-007–0967-2
11. Kulkarni K, Chang ZH, Lei ST (2004) Surface micro/nanostructuring of cutting tool materials by femtosecond laser. Trans North Am Manuf Res Inst SME 32:25–32
12. Mannion PT, Magee J, Coyne E, O'Connor GM, Glynn TJ (2004) The effect of damage accumulation behaviour on ablation thresholds and damage morphology in ultrafast laser micro-machining of common metals in air. Appl Surf Sci 233:275–278 DOI 10.1016/j.apsusc.2004.03.229